ADVANCES IN ATMOSPHERIC SCIENCES, VOL. 24, NO. 1, 2007, 101–110

An Algorithm on Convective Weather Potential in the Early Rainy Season over the Pearl River Delta in China

FENG Yerong*[1,2] (冯业荣), WANG Ying[1] (汪 瑛), PENG Taoyong[1] (彭涛涌), and YAN Jinghua[3] (闫敬华)

[1] *Department of Atmospheric Sciences, Zhongshan University, Guangzhou* 510270

[2] *Guangdong Meteorological Observatory, Guangzhou* 510080

[3] *Guangzhou Institute of Tropical and Marine Meteorology, China Meteorological Administration, Guangzhou* 510080

(Received 11 July 2005; revised 9 June 2006)

ABSTRACT

This paper describes the procedure and methodology to formulate the convective weather potential (CWP) algorithm. The data used in the development of the algorithm are the radar echoes at 0.5° elevation from Guangzhou Doppler Radar Station, surface observations from automatic weather stations (AWS) and outputs of numeric weather prediction (NWP) models. The procedure to develop the CWP algorithm consists of two steps: (1) identification of thunderstorm cells in accordance with specified statistical criteria; and (2) development of the algorithm based on multiple linear regression. The thunderstorm cells were automatically identified by radar echoes with intensity greater than or equal to 50 dB(Z) and of an area over 64 square kilometers. These cells are generally related to severe convective weather occurrences such as thunderstorm wind gusts, hail and tornados. In the development of the CWP algorithm, both echo- and environment-based predictors are used. The predictand is the probability of a thunderstorm cell to generate severe convective weather events. The predictor-predictand relationship is established through a stepwise multiple linear regression approach. Verification with an independent dataset shows that the CWP algorithm is skillful in detecting thunderstorm-related severe convective weather occurrences in the Pearl River Delta (PRD) region of South China. An example of a nowcasting case for a thunderstorm process is illustrated.

Key words: convective weather potential, nowcasting, Doppler radar, mesoscale numerical model

DOI: 10.1007/s00376-007-0101-2

1. Introduction

Other than precipitating weather, the severe convective weather occurrences in this paper refer to severe convective ones such as strong wind gusts, hail and tornados that are induced by thunderstorms. The nowcasting of these severe convective weather occurrences is difficult because of their abruptness with strong intensity and short duration. At present, the development of a nowcasting technique for severe convective weather occurrences is focused on three aspects: (1) the development of the techniques for identification, tracking and extrapolation of a thunderstorm cell (denoted as a storm cell for short) (Rinehart, 1981; Dixon and Wiener, 1993; Brown and Brandes, 1997); (2) development of mesoscale or storm-scale numerical weather prediction models (Xue et al., 2003); and (3) development of conceptual models for interpretation combining both (1) and (2) (Wilson and Mueller, 1993; Wilson et al., 1998; Mueller et al., 2003; Wilson et al., 2004). Among them, the development of conceptual models for interpretation is the mainstream of technical development of nowcasting techniques in many countries (Chen et al., 2004). Such interpretation techniques are generally incorporated with a variety of meso- or micro-scale observations including radar and satellite data to develop conceptual models for the initiation, growth and dissipation of thunderstorms. These conceptual models integrate numerical weather prediction (NWP) model outputs and other extrapolation products to build the nowcasting system of thunderstorms by means of statistical interpretation approaches. Many operational applications have showed that these interpretation nowcasting

*E-mail: yerong_feng@yahoo.com

models/systems usually outperform other techniques with more accuracy and longer lead time. In recent years, such nowcasting systems have been developed at many institutions, for instance, the ANC (AutoNowcaster) (Mueller et al., 2003) by the U. S. National Center for Atmospheric Research (NCAR), the GANDOLF (Generating Advanced Nowcasts for Deployment in Operational Land Surface Flood Forecast) (Pierce et al., 2000) by the U. K. Met Office, the SCAN (System for Convective Analysis and Nowcast) (Smith et al., 1998) by the U.S. National Weather Service (NWS), and the SWIRLS (Short-range Warning of Intense Rainstorms in Localized System) by the Hong Kong Observatory (Li et al., 2000)

Studies on nowcasting of mesoscale severe weather events have been carried out in China in recent years. Wang and Ding (1994) analyzed the collocation of mesoscale systems associated with hail phenomena in Beijing and proposed a conceptual model for identifying the hail zone. Ding et al. (1996) used helicity as a dynamical parameter in the severe weather forecasting. Based on atmospheric dynamics, moisture, stability and triggering mechanisms, Du and Guan (2000) developed a nowcasting system for severe convective weather phenomena in Shanghai using outputs of mesoscale numerical models, Doppler radar observations, geostationary satellite observations, MICAPS (Meteorological Information Combined Analyses and Processing System), and the automated precipitation observation network, in combination with forecasters' experience. The system has proven effective in nowcasting severe weather events in Shanghai.

In recent years, the rapid improvement of observation techniques, data communication facilities and mesoscale numerical prediction models in China has provided advanced means to develop operational systems for objective and quantitative nowcasting of thunderstorms.

The Pearl River Delta (PRD) is an area with frequent occurrences of severe convective weather phenomena in the early rainy season (ERS) which starts from April till June each year. Many studies have focused on the convective processes in this area. Luo et al. (1994) conducted detailed studies on the local severe storms in the PRD and obtained much improved understanding on the behaviors of thunderstorms. Xu (1994) analyzed the meteorological conditions that triggered the occurrence of a severe convective weather process in the region covered by a subtropical high. Wang (1994) concluded that the local storms were apt to be generated under the conditions of low pressure at the surface, when it is unstable and much warmer in the lower layers and much more humid in the whole troposphere. Liu et al. (2001) described the characteristics of severe convective processes initiated by a sea breeze front. These studies revealed that the initiation and development of a severe convective weather process in the PRD region are closely related to the larger-scale dynamic and thermodynamic conditions of the atmosphere. Therefore in our study, not only variables derived on the basis of radar echoes but also parameters provided by mesoscale numerical weather prediction models are incorporated into the nowcasting algorithm.

2. Dataset

The Guangzhou next-generation Doppler radar situated at 23.004°N, 113.355°E was put into operation in 2001. The radar is able to provide volumetric scanning capability for the whole PRD region every 6 minutes. In this study, imageries of radar reflectivity for a 230-km scanning radius at a 0.5° elevation angle were collected during April–June 2004. The echo intensities are subdivided into 15 categories with different values assigned according to the reflectivity, e.g., 1 is assigned to category one, whose reflectivity range is 1–5 dB(Z); 2 was assigned to category two whose reflectivity range is 6–10 dB(Z); and so on. The echo intensity data on a $1^\circ \times 1$ km grid mesh were derived from each reflectivity image along the azimuth ranging from 1° to 360° and radius ranging from 1 to 230 km, forming a dataset with a total of 360×230 pixels on a given radar image.

In the last five years, more than 600 automatic weather stations (AWSs) spaced roughly 10–20 km apart have been deployed in the Guangdong Province. Most of the AWSs observe four meteorological variables (wind speed, wind direction, temperature, and precipitation), while others observe six meteorological variables (air pressure and humidity in addition to the other four variables), and the AWS observations are reported every 6 minutes.

In this study, a severe convective weather event was defined as either a wind gust greater than or equal to 17 m s^{-1} observed at an AWS station, a hail report of any size or a report of a tornado. The hail and tornado reports were based on local field observations. The likelihood is high that a large majority of the severe weather events was reported because of the high population density and the relatively close spacing of the AWS stations. Small-scale wind phenomena like microbursts may have gone unreported. A total of 358 severe convective weather events were recorded during April–June 2004 within the 230-km range of Guangzhou radar. These severe convective weather events were comprised of 354 wind gust events, 3 hail events and 1 tornado event. The wind gust events dominated by taking up 98.9% of the whole severe con-

vective weather samples, while the hail and tornado events were extremely rare, taking up only 0.84% and 0.28% of them, respectively. Hail and tornado reports were carefully confirmed by meteorological agencies to maintain reliability.

Environmental predictors were obtained from numerical weather prediction (NWP) model products. These environmental variables were derived from 12–36-h forecasts of the mesoscale numerical prediction model by the Guangzhou Institute of Tropical and Marine Meteorology, China Meteorological Administration (CMA) (denoted as the GZHM model), as archived by the Guangdong Meteorological Observatory. The GZHM model is a mesoscale non-hydrostatic model that runs two times per day (0000, 1200 UTC). The model has a spatial resolution of 14 km and the results were output hourly from 12 to 36 hours during the model integration. The model values assigned to a storm cell were those of the closest model grid point.

3. Storm cell identification and cell-event correspondence

The process for developing the CWP algorithm includes three steps: (1) identification of an individual convective storm cell; (2) determination of cell-event correspondence, and (3) development of a nowcast algorithm to provide the probabilities of cell-produced severe convective weather events.

Firstly, a storm cell was defined by a radar echo with a reflectivity reaching a specified intensity (intensity threshold) and areal size (spatial threshold). In the algorithm, each such storm cell can be automatically identified on a reflectivity image. Previously Kitzmiller and Saffle (1995), in their development of similar severe weather potential algorithms, defined a storm cell as a VIL (Vertically Integrated Liquid) of 10 kg m^{-3} over at least two contiguous 4 km×4 km grid points. In the present investigation, a storm cell is defined as a radar echo having a reflectivity greater than or equal to 50 dB(Z) (intensity threshold) and the cell covers an area of 64 km^2. The definition of a cell covering 64 square kilometers is similar to requiring that a storm cell should be at least 8 km in length. This size approximately approaches the lower limit of the average spatial scale for an individual thunderstorm cell (10 to 30 km), as defined by Byers and Braham (1949).

Secondly, each storm cell identified in the first step should be defined whether or not it was severe. An individual storm cell was defined as severe if at least one severe weather report occurred within 60 km of the cell centroid and within one hour. If multiple cells met this criteria, the cell closest in time and space was assigned the severe status. Thus we established a correspondence between an observed severe convective weather event and a storm cell.

It should be pointed out that the proper combination of spatial and intensity thresholds is needed to reasonably identify a cell to avoid over-identifying severe thunderstorm cells. An optimal threshold combination should be such that it should increase the ratio of the number of event-corresponding cells to the total number of cells identified, viz., the event-detection ratio. Listed in Table 1 are several threshold combinations for the data in April 2004. Different spatial and intensity threshold combinations may result in significant difference in the number of cells identified. The last row indicates the threshold combination that produces the largest event detection ratio. So this threshold combination (reflectivity $\geqslant$50 dB(Z) and area $\geqslant$64 km^2) was used in this study to define a storm cell. Such a cell identification approach resulted in 1064 cells in April 2004, of which 32 could bring in severe convective weather events.

Thirdly, in order to generate the predictor-predictand dataset needed in the development of the algorithm, it is necessary to keep the sampling procedure statistically reliable. Storm cells occurring over the sea were excluded from the dataset because the corresponding severe convective weather events could not be observed.

As can be seen from the above, the event detection ratio is so low that it is impossible to nowcast severe convective weather phenomena only by the identified cells. Severe thunderstorms are strong convective systems that developed in a specific atmospheric environment, e.g. boundary layer convergence, or an unstable and humid atmosphere (Crook, 1996; Mueller et al., 2003). Environmental parameters that reflect atmospheric dynamic or thermodynamic effects on thunderstorm development should be important in the diagnosis of the initiation, growth and dissipation of the storm cells and in predicting the types of convective events (Li et al., 2004; Wilson and Mueller, 1993). Therefore, these environmental variables must be considered in the nowcasting problem of severe convective weather.

The number of identified cells in the ERS months over the PRD region in 2004 is shown in the second column in Table 2, while the corresponding number of severe convective weather events is provided in the third column. The fourth column shows the number of cell-related events, i.e., the severe convective weather events produced apparently by the storm cells. And the fifth column shows the number of severe convec-

Table 1. Event detection ratios from different combinations of cell identification thresholds.

Cell intensity [dB(Z)]	Cell size (km^2)	No. of identified cells	No. of event-corresponding cells	Event detection ratio
$\geqslant 40$	$\geqslant 81$	6135	45	0.007
$\geqslant 45$	$\geqslant 81$	2895	39	0.013
$\geqslant 40$	$\geqslant 100$	5117	44	0.009
$\geqslant 45$	$\geqslant 100$	2326	39	0.017
$\geqslant 45$	$\geqslant 90$	2599	39	0.015
$\geqslant 50$	$\geqslant 64$	1064	32	0.030

Table 2. Statistics on cell identification and the cell-event relationship.

Month	No. of identified cells	No. of severe weather events	No. of cell-relevant events	No. of cell-irrelevant events	Event exclusion ratio
April	1064	36	32	4	0.11
May	918	197	160	37	0.19
June	726	125	101	24	0.19

tive weather events that are not related to an identified thunderstorm cell. This may arise when cells <50 dB(Z) and <64 km^2 in size produce severe weather. As shown in the last column of Table 2, as many as 19% of the severe weather events were not associated with a cell >50 dB(Z) and 64 km^2 in size. This means that more than 80% of the events were cell-related, namely, produced by thunderstorm cells. Only less than 20% of the events had been found cell-irrelevant or missed by the cell identification limitation and were excluded from the dataset.

Figure 1a shows the ratios of the number of severe convective weather events to that of identified cells during the ERS months. These ratios are 3%, 17.4%, and 13.9% for April, May and June 2004, respectively. Due to the low ratios, we could not get much worthy information about the severe weather occurrence from cell identification. A great portion of the identified cells accounted for precipitation, thus only a small proportion of the convective echoes reported severe weather. Therefore, the direct application of convective echoes to nowcast severe weather would only lead to unacceptable, high false-alarm ratios. Figure 1b shows the proportion of convective events that were found cell-relevant. More than 80% of convective weather events could be detected by radar through thunderstorm cell identification. Only a small proportion of cells were missed owing to the limitation inherent in the cell identification approach.

4. Convective weather potential algorithm

It is obvious that most of the thunderstorm cells on the radar images produced precipitation. Only a small proportion of them, however, could produce severe convective weather events. The purpose of the CWP algorithm is to identify those radar echoes containing severe weather. The dataset for statistical analysis was subdivided into two subsets: a dependent or development one, and an independent or verification one. The dependent dataset consisted of two thirds of the samples derived from the original dataset through a random-selection procedure. This subset was used to develop the CWP algorithm through a multiple linear regression process. The independent dataset was composed of the remaining one third of the data samples. This subset was analyzed to evaluate the algorithm performance. A total of 30 candidate predictors was applied to a stepwise multiple linear regression process to obtain a linear expression of probabilities for severe convective weather occurrences. The details of these candidate predictors are listed in Table 3. Twenty-six of the predictors are environment-based parameters describing environmental flow characteristics and instability. Four of them are cell-based predictors mainly from reflectivity features. The VIL values were customarily found less accurate and apparently weak, especially when the echo system was moving fast. So they were not considered in the algorithm for the time being. Radar radial velocity was also excluded due to the lack of an effective way to remove the frequently-occurring ambiguity in the velocity product.

Originally there were 2708 storm cells obtained from radar reflectivity imageries during April–June 2004. Due to the lack of acquired NWP model data and no convective weather records available over the sea, only a set of 1513 cell samples were available, in which two thirds of the cases (1010) were used for the

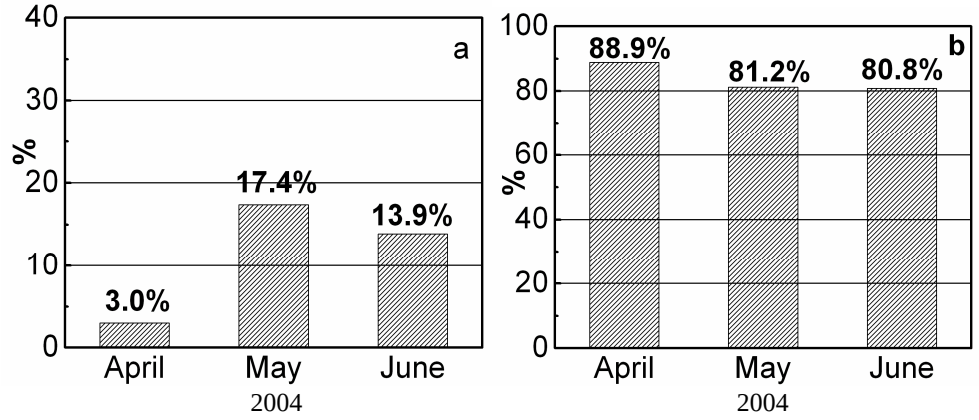

Fig. 1. (a) Ratios of events to cells; (b) proportion of cell-relevent severe convective weather events.

development dataset. The other one third of the cases (503) were used for the verification dataset.

In the CWP algorithm, the predictand represents the probability of severe convective weather occurrence produced by an individual storm cell. The value of the predictand was normalized according to the cell-event correspondence. If a correspondence existed, the predictand was assigned to the value unity. Otherwise, it was assigned zero.

The selection procedure of predictors through the stepwise multiple linear regression yielded the following algebraic relationship between the available predictors and event probability:

$$\begin{aligned} \mathrm{CWP} =& 8.53 + 0.0593 \times \mathrm{REFLTY} - 0.0022\times \\ & \mathrm{CAREA55} - 1273.07 \times \mathrm{DIV}_{850} + 1158.06\times \\ & \mathrm{VOR}_{500} - 0.0616 \times T_{500-200} - 0.011\times \\ & v_{500-850} - 0.030 \times V_{850} - 0.033 \times V_{500} + \\ & 0.018 \times u_{700} + 0.024 \times u_{500} + 0.0034\times \\ & \mathrm{RH}_{850+700+500} + 0.022 \times K_{\mathrm{i}} - \\ & 0.0085 \times \mathrm{LCL}\ . \end{aligned} \tag{1}$$

The above expression produces the convective weather potential which represents the probability of a storm cell to generate severe convective weather phenomena within an area not exceeding 60 km in range from an echo center in a very short period of time (1 hour). As indicated in Eq. (1), 13 predictors were introduced by the stepwise linear regression. These predictors include variables that describe storm characteristics and environmental conditions for the storm. They are maximum reflectivity of the cell (REFLTY), area of the cell with reflectivity $\geqslant$55 dB(Z) (CAREA55), divergence at 850 hPa (DIV_{850}), vorticity at 500 hPa (VOR_{500}), temperature difference between 200 and 500 hPa ($T_{500-200}$), vertical shear of the v-component between 500 and 850 hPa ($v_{500-850}$), wind speed at 850 hPa (V_{850}), wind speed at 500 hPa (V_{500}), u-component of wind at 700 hPa (u_{700}), u-component of wind at 500 hPa (u_{500}), mean relative humidity in the lower layer ($\mathrm{RH}_{500+700+850}$), K index (K_{i}) and lifting condensation level (LCL). The predictors in equation (1) indicate that storm cells are more likely to produce severe convective weather phenomena in situations with strong reflectivity, high upper-layer thermal instability, relatively humid lower layer air, strong mid-tropospheric zonal winds, strong mid-tropospheric vorticity, strong lower layer convergence and generally strong vertical shear of the meridional component of wind, etc.

The process that generated equation (1) experienced a number of trials. Note that the multiple linear relationship between predictand and predictors was established through a stepwise linear regression. The result of the regression could be quite dependent on the development sample. In the stepwise regression, each candidate predictor is included into or removed from the regression equation according to its variance contribution, depending on whether or not it passes the level of significance for the F-statistic. We tried to find the best possible regression equation from 100 sets of exploratory samples which were randomly selected for the development dataset, in an effort to achieve the highest critical success index (CSI) (which will be defined later). Table 4 shows the results from the stepwise regression procedure. The second column in the right panel indicates the number of times that each predictor is selected in the stepwise analysis. For 100 trials, LCL was the only variable that was selected every time. In other words, the lifting condensation level was the most sensitive predictor in all candidate predictors. Other frequently-selected predictors were REFLTY, $T_{500-200}$, $\mathrm{RH}_{850+700+500}$, CAREA 55,

Table 3. Candidate predictors for the convective weather potential.

Environment-based predictors from the model:	
V_{850} , V_{700}, V_{500}	Wind speed at 850, 700 and 500 hPa, respectively, in m s^{-1}
u_{850}, u_{700}, u_{500}, u_{200}	u-component of wind at 850 , 700, 500 and 200 hPa, respectively, in m s^{-1}
v_{850}, v_{700}, v_{500}, v_{200}	v-component of wind at 850 hPa, 700, 500 and 200 hPa, respectively, in m s^{-1}
$u_{500-850}$, $u_{200-500}$	u-component wind shear between 500 and 850 hPa, and 200 and 500 hPa, respectively, in m s^{-1}
$v_{500-850}$, $v_{200-500}$	v-component wind shear between 500 and 850 hPa, and 200 and 500 hPa, respectively, in m s^{-1}
DIV$_{850}$, DIV$_{500}$	Divergence at 850 and 500 hPa, respectively, in s^{-1}
VOR$_{500}$	Vorticity at 500 hPa, in s^{-1}
$T_{850-500}$	Temperature departure between 850 hPa and 500 hPa, in °C
$T_{500-200}$	Temperature departure between 500 hPa and 200 hPa, in °C
RH$_{850+700+500}$	Mean relative humidity at 850, 700 and 500 hPa, in %
TOTALS	Total totals index ($=T_{850}+TD_{850}-2T_{500}$), in °C
$K_{\rm i}$	K index [$=T_{850}-T_{500}+TD_{850}-(T_{700}-TD_{700})$], in °C
CAPE	Convective available potential energy, in J kg^{-1}
SI	Showalter index, in °C
LCL	Lifting condensation level, in m
Cell-based predictors from the radar:	
REFLTY	Maximum intensity of the radar echo of a cell, in dB(Z)
CAREA50	Areas of reflectivity $\geqslant$50, 55 or 60 dB(Z), respectively,
CAREA55	within a cell, in km^2
CAREA60	

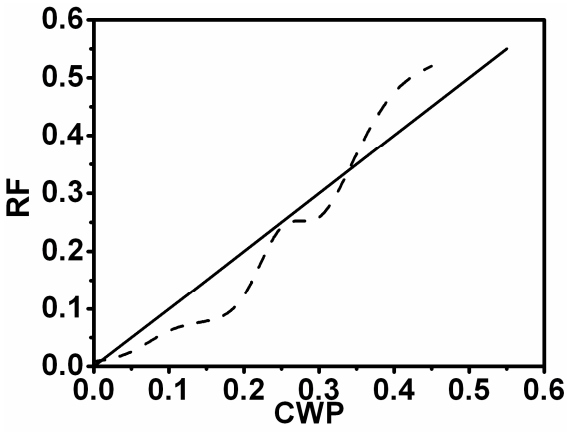

Fig. 2. Observed relative frequency of severe convective weather occurrences as a function of forecasted probability.

DIV$_{850}$ and V_{850}. Though CAPE is often thought to be critical in thunderstorm forecasts (Rasmussen and Blanchard, 1998; Blanchard, 1998), it was less frequently selected in our trials and finally excluded from the best-fit equation.

The standard error STEYX measures the amount of error in the prediction of the predictand for an individual predictor in the regression. It is defined by:

$$\mathrm{STEYX} = S_y\sqrt{\frac{1}{n-2}(1-R_{xy}^2)}\,, \qquad (2)$$

where S_y is the standard deviation of predictand y, n is the sample size, and R_{xy} is the correlation coefficient between predicted variable y and predictor x. Equation (2) represents the independent contributions of each predictor to the prediction of the predictand.

As shown in the third column in Table 4, the standard error related to LCL is the lowest of all predictors, with an accompanying highest value of R_{xy}^2 (last column). These results reveal that LCL is the most contributory parameter. It accounts for most of the regression variance and reduces the standard error.

Though some parameters such as REFLTY and DIV$_{850}$, etc., have small correlation coefficients, they were introduced into the regression equation by stepwise analysis. This is because they have significant contributions in conjunction with other predictors in the equation. Though individually some predictors such as V_{700} and u_{850} showed high correlation with the predictand, they were not significant enough to be

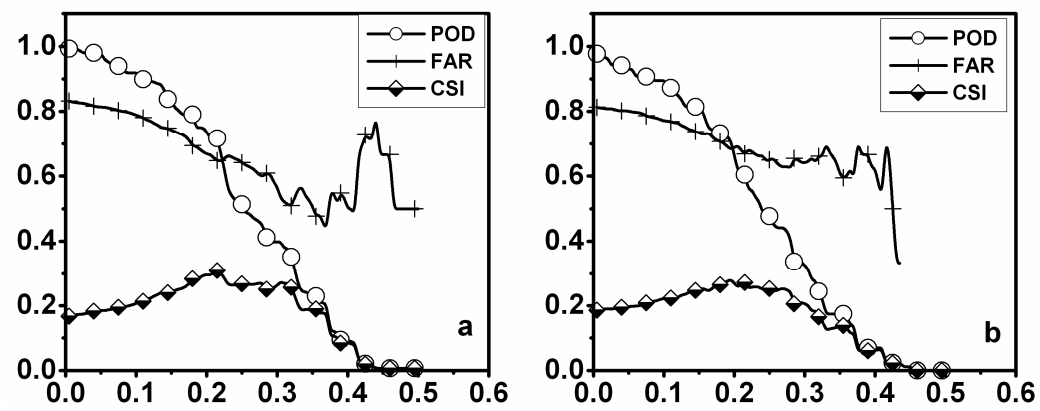

Fig. 3. The variation of POD, FAR and CSI with respect to CWP probability threshold. (a) for dependent dataset; (b) for independent dataset.

accepted into the regression equation when they worked together with other predictors.

5. Performance of the algorithm

The output of the CWP algorithm is the probability or potential of severe convective weather occurrence for an individual cell. To test the statistical reliability of the algorithm, an evaluation was made on the dependent dataset. The observations of severe convective weather were used to verify the probability over every 10% interval to see how closely the average forecasted probability approximated the relative frequency (RF) of actual events. In Fig. 2, the observed RF is plotted as a function of the mean forecasted probability. The solid line represents perfect reliability. The CWP forecasted probability varies closely to the perfect reliability criterion for most probability ranges. Overall, in the lower probability range 0%–35%, the RF of convective weather occurrences tends to be lower than the CWP forecasted probability. While in the upper probability range >35%, the RF of convective weather events tends to be higher than the CWP forecasted probability.

Though the CWP algorithm provides a probabilistic forecast, its performance is most easily evaluated by examining the yes/no (severe convective weather/precipitation) forecasts based on the probabilities. The yes/no forecasts are generally derived through setting a fixed threshold probability value, and forecasting all storm cells with probabilities at or above the threshold to produce severe convective weather.

The performance of the yes/no forecasts may be described by three commonly-used measures, the probability of detection (POD), false alarm ratio (FAR), and critical success index (CSI) (Donaldson et al., 1975; Schaefer, 1990). Let x be the number of severe thunderstorm cells correctly forecasted to be severe, y the number of severe thunderstorm cells incorrectly forecasted to be non-severe (i.e., the precipitating cells), and z the number of non-severe cells incorrectly forecasted to be severe. Then the scores are defined by Probability of Detection (POD):

$$\mathrm{POD} = x/(x+y)\ . \tag{3}$$

False Alarm Ratio (FAR):

$$\mathrm{FAR} = z/(x+z)\ . \tag{4}$$

Critical Success Index (CSI):

$$\mathrm{CSI} = x/(x+y+z)\ . \tag{5}$$

The performance of the CWP algorithm in terms of POD, FAR and CSI is shown in Fig. 3. These scores were from a sample of cases for the development dataset (a) and the verification dataset (b).

For the dependent dataset, CWP varies within the range 0.0–0.5. As has been shown, the yes/no forecast skill is highly dependent on the CWP threshold. If the threshold of the CWP value is set very high, not enough severe convective weather occurrences would be forecasted and the POD would be rather low. However, if the threshold is set too low, too many false alarms would be issued. The optimal choice may be setting the threshold at a point where the CSI remains high while achieving an acceptable, high POD and relatively low FAR. The point is found at the place where the CSI is as close as possible to the peak. For example, when using 0.195 as the CWP threshold probability, about 75% of the severe convective weather events were detected (POD=0.75), and 67% of the "yes" fore-

Table 4. The statistical parameters denoting the performance of the linear regression.

Predictor	No. of times introduced	Standard error	R_{xy}^2
Predictors being introduced into the regression equation			
LCL	100	0.0958	0.4371
REFLTY	94	0.1244	0.0084
$RH_{850+700+500}$	92	0.1214	0.0971
$T_{500-200}$	92	0.1239	0.0357
CAREA55	86	0.1246	0.0473
DIV_{850}	83	0.1273	0.0055
V_{850}	73	0.1032	0.3516
$v_{500-850}$	56	0.1241	0.0154
u_{700}	43	0.1130	0.2045
V_{500}	25	0.1123	0.1772
VOR_{500}	24	0.1273	0.0051
$K_{\rm i}$	15	0.1188	0.1034
u_{500}	7	0.1165	0.1224
Predictors without being introduced into the regression equation			
u_{850}	48	0.1087	0.2756
CAREA60	39	0.1271	0.0103
CAPE	37	0.1232	0.0689
v_{500}	35	0.1228	0.0750
V_{700}	26	0.1056	0.3163
DIV_{500}	16	0.1210	0.1024
$u_{200-500}$	16	0.1248	0.0207
u_{200}	16	0.1212	0.0997
v_{700}	15	0.1203	0.1128
v_{850}	12	0.1207	0.1071
$u_{500-850}$	10	0.1264	0.0207
$v_{200-500}$	9	0.1256	0.0329
$T_{850-500}$	8	0.1241	0.0565
CAREA50	7	0.1268	0.0139
v_{200}	5	0.1211	0.1005
TOTALS	5	0.1194	0.1265
SI	3	0.1181	0.1455

casts were false alarms (FAR=0.67). The CSI at that threshold probability was 0.294. It should be mentioned again that the peak CSI value is also an indicator for the stepwise regression process to decide which set of development samples is the best, as was discussed in section 4.

For the independent dataset, the results are similar. If a threshold value of 0.195 is applied, the CSI reaches 0.28. The POD obtains a value of 0.71. The FAR is 0.68. These results indicate that the CWP algorithm is statistically rather robust.

An example of severe weather nowcasting using the CWP algorithm is shown in Fig. 4. On the radar reflectivity imagery at 1620 LST 16 May 2004, there were four thunderstorm cells detected by the storm cell identification process. The CWP algorithm yielded valves of 0.35, 0.31, 0.225, and 0.19 for these cells, respectively. Three storm cells were forecasted to produce severe convective weather events within 1 hour, since their CWP values exceeded the probability threshold of 0.195. The other one was forecasted not to produce severe convective weather, as its CWP value was less than the probability threshold. Two severe convective weather events were correctly forecasted, as indicated by the cross signs in Fig. 4. They were wind gusts happening at Sanshui and Heyuan Prefectures. One false alarm was issued. And the cell with CWP less than the threshold was also successfully forecasted to be a non-severe one. Therefore, the CWP algorithm made satisfactory nowcasts for this convective weather process.

6. Summary

A convective weather potential algorithm was developed in this study. The algorithm is capable of providing the probability of a storm cell to generate severe convective weather events.

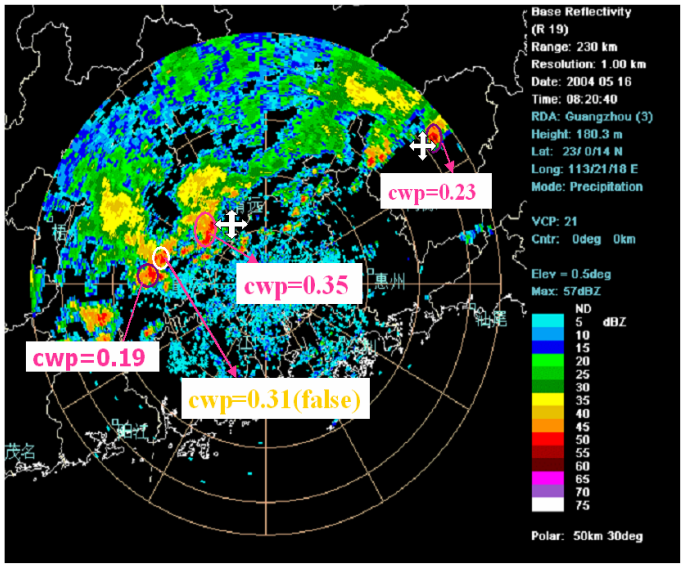

Fig. 4. An example of a nowcasting severe convective weather based on a probability threshold of 0.195. The cross signs indicate the observed wind gusts.

A storm cell was defined as a radar echo having a reflectivity greater than or equal to 50 dB(Z) where the cell covers an area of at least 64 km^2. This cell definition could identify thousands of thunderstorm cells during the ERS in 2004 over the PRD region of South China. Most of these storm cells were associated with precipitation. Only a very small proportion of them (about less than 18%) were related to severe convective weather events. Though the storm cells that could produce severe convective weather are rare, over 80% of such cells could be captured by the cell identification algorithm.

The CWP represents the probability of a thunderstorm cell to generate a severe convective weather event. This CWP was developed through a stepwise multiple linear regression approach based on both radar-based and NWP-based predictors. The CWP was a best-fit equation produced through 100 different subsets of data samples that were randomly formed. Verification of the CWP algorithm was conducted for both dependent and independent datasets based on a yes/no forecast through setting a certain probabilistic threshold. This probabilistic threshold was determined to obtain as high as possible a CSI value for the development dataset. For the independent dataset, the CWP yielded a CSI of 0.28 and a POD of 0.71 when using a threshold value of 0.195, while keeping a tolerant FAR of 0.68.

Though verification of the performance of the CWP algorithm for both dependent and independent samples and a nowcasting case showed that the algorithm was skillful in nowcasting convective weather occurrences, further improvement is still needed. Introduction of a more or less subjective definition of a thunderstorm cell resulted in a few severe convective weather cases being excluded from the statistical sampling because their relevant cells were too small or too weak to be automatically detected through the pre-determined threshold criteria. This led to the state that about 19% of the severe convective weather events were excluded from the sample dataset. A more effective cell identification approach is expected to be developed in order to keep as many severe convective weather samples as possible in the development dataset.

With the development and deployment of other unconventional facilities such as geostationary satellites, wind profilers, lightning ranging systems and Global Positioning System (GPS) moisture monitoring instruments, the CWP algorithm is expected to be improved by incorporating these data as much as possible. Other radar products such as Vertically Integrated Liquid (VIL) and radar radial velocity may also be incorporated into the algorithm in the future as the quality of data is improved.

Acknowledgements. This work was funded by the Ministry of Science and Technology of China, under the project of research on the monitoring and warning techniques for the convective weathers in the Pearl River Delta region (Grant 2003DIB4J145), by the Grant No. CMATG2005Y04 from China Meteorological Administration, and by the Grant No. 2006A02 from Guangdong Meteorological Bureau.

REFERENCES

Blanchard, D. O., 1998: Assessing the vertical distribution of convective available potential energy. *Wea. Forecasting,* **13**, 870–877.

Brown, B. G., and E. Brandes, 1997: An intercomparison of 2D storm motion extrapolation algorithms. *Preprints, 28th Conf. on Radar Meteorology*, Austin, TX, Amer. Meteor. Soc., 495–496.

Byers, H. R., and R. R. Braham Jr., 1949: *The Thunderstorm*. U. S. Department of Commerce, Weather Bureau, 287pp.

Chen Mingxuan, Yu Xiaoding, Tan Xiaoguang, and Wang Yingchun, 2004: A brief review on the development of nowcasting for convective storms. *Journal of Applied Meteorological Science*, **15**, 754–766. (in Chinese)

Crook, N. A., 1996: Sensitivity of moist convection forced by boundary layer processes to low-level thermodynamic fields. *Mon. Wea. Rev.*, **124**, 1767–1785.

Ding Jincai, Dai Jianhua, Chen Yaming, Hu Fuquan, and Tang Xinzhang, 1996: Helicity as a method for forecasting severe weather events. *Adv. Atmos. Sci.*, **13**, 533–538.

Dixon, M., and G. Wiener, 1993: TITAN: Thunderstorm Identification, Tracking, Analysis, and Nowcasting—A radar-based methodology. *J. Atmos. Oceanic Technol.*, **10**, 785–797.

Donaldson Jr., R. J., R. M. Dyer, and J. J. Kraus, 1975: An objective evaluator of techniques for predicting severe weather events. *Preprints, Ninth Conference on Severe Local Storms*, Amer. Meteor. Soc., Norman, 321–326.

Du Bingyu, and Guan Li, 2000: Nowcasting system of severe convective weather in Shanghai. *Journal of Nanjing Institute of Meteorology*, **23**, 242–250. (in Chinese)

Kitzmiller, D. H., and R. E. Saffle, 1995: The WSR-88D severe weather potential algorithm. *Wea. Forecasting*, **10**, 141–159.

Li, P. W., W. K. Wong, K. Y. Chan, and S. T. Lai Edwin, 2000: SWIRLS—An evolving nowcasting system. *Technical Note*, No. 100, Hong Kong Observatory, 33pp.

Li Yaodong, Liu Jianwen, and Gao Shouting, 2004: On the progress of application for dynamic and energetic convective parameters associated with severe convective weather forecasting. *Acta Meteorological Sinica*, **62**, 401–409. (in Chinese)

Liu Yunce, Zhuang Xudong, and Li Xianzhou, 2001: Severe local storms initiated by the sea breeze front in the Pearl River Delta during the late spring and summer. *Journal Of Applied Meteorological Science*, **12**, 433–441. (in Chinese)

Luo Huibang，He Haiyan, Wu Chisheng, and Lin Yinghe, 1994: *The Local Severe Storm in the Pearl River Delta*, Sun Yatsen University Press, 153pp. (in Chinese)

Mueller, C., T. Saxen, R. Roberts, J. Wilson, T. Betancourt, S. Dettling, N. Oien, and J. Yee, 2003: NCAR auto-nowcast system. *Wea. Forecasting*, **18**, 545–561.

Pierce, C. E., C. G. Collier, P. J. Hardaker, and C. M. Haggett, 2000: GANDOLF : a system for generating automated nowcasts of convective precipitation. *Meteorol. Appl.*, **7**, 341–360.

Rasmussen, E. N., and D. O. Blanchard, 1998: A baseline climatology of sounding-derived supercell and tornado forecast parameters. *Wea. Forecasting*, **13**, 1148–1164.

Rinehart, R. E., 1981: A pattern recognition technique for use with conventional weather radar to determine internal storm motions. *Atmos. Technol.*, **13**, 119–134.

Schaefer, J. T., 1990: The critical success index as an indicator of warning skill. *Wea. Forecasting*, **5**, 570–575.

Smith, S. B., J. T. Johnson, R. D. Roberts, S. M. Zubrick, and S. J. Weiss, 1998: The system for convective analysis and nowcasting (SCAN): 1997–1998 field test. *Preprints, 19th Conf. on Severe Local Storms*, Minneapolis, MN, Amer. Meteor. Soc., 790–793.

Wang Peilin, 1994: On the genesis conditions of severe local storms in the Pearl River Delta. *Acta Meteorologica Sinica*, **52**, 252–256.

Wang Xiaofang, and Ding Yihui, 1994: Study on method of short-range forecast of severe convective weather in Beijing area. *Scientia Atmospherica Sinica*, **18**, 173–183. (in Chinese)

Wilson, J. W., and C. K. Mueller, 1993: Nowcasting thunderstorm initiation and evolution. *Wea. Forecasting*, **8**, 113–131.

Wilson, J. W., N. A. Crook, C. K Mueller, Juanzhen Sun, and Michael Dixon, 1998: Nowcasting thunderstorm: A status report. *Bull. Amer. Meteor. Soc.*, **79**, 2079–2099.

Wilson, J. W., R. Roberts, and C. Mueller, 2004: Sydney 2000 forecast demonstration project: Convective Storm Nowcasting. *Wea. Forecasting*, **19**, 131–150.

Xu Lizhang, 1994: Diagnostic analysis on physical variant fields of one strongly convective weather process over the Delta of Pearl River. *The Journal of Sun Yatsen University* (Suppl.), **5**, 46–49. (in Chinese)

Xue, M., D.-H. Wang, J.-D. Gao, K. Brewster, and K. K. Droegemeier, 2003: The Advanced Regional Prediction System (ARPS), storm-scale numerical weather prediction and data assimilation. *Meteor. Atmos. Phys.*, **82**, 139–170.